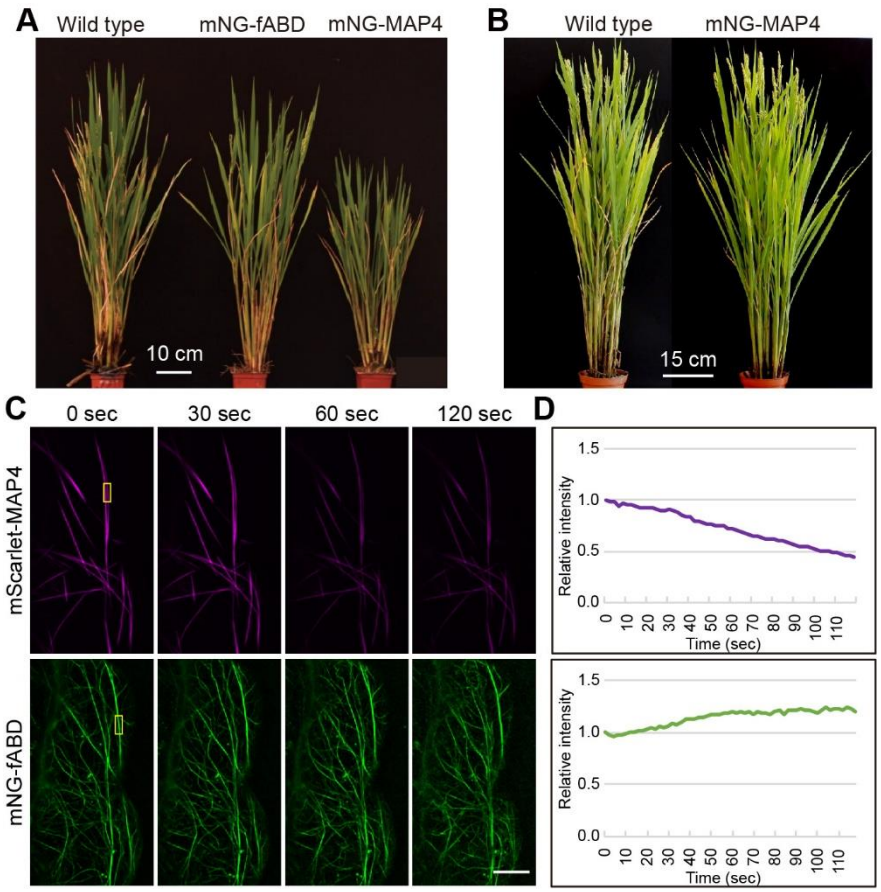

Fig. S1. The plant phenotype and photo-bleaching of RUBQ driving lines. (A-B) The transgenic plant phenotype of *mNG-fABD* and *mNG-MAP4* lines. The *mNG-fABD* lines are indistinguishable from the wild-type plants. Some *mNG-MAP4* lines can cause plant dwarf phenotype (A) while some normal lines as in (B) can also be obtained. (C) Bleaching test for the fluorescent proteins. The images were from a time lapse stack taken from the coleoptile epidermis of dual labelled line *RUBQ2::mScarlet-MAP4 RUBQ2::mNG-fABD (mScarlet-MAP4 mNG-fABD* in short*)*. The duration was 2 min with 2 sec time interval. Note the quick intensity decrease of the mScarlet channel. Scale bar: 10 μm. (D) Fluorescent signal plot of the yellow rectangle regions in (C).

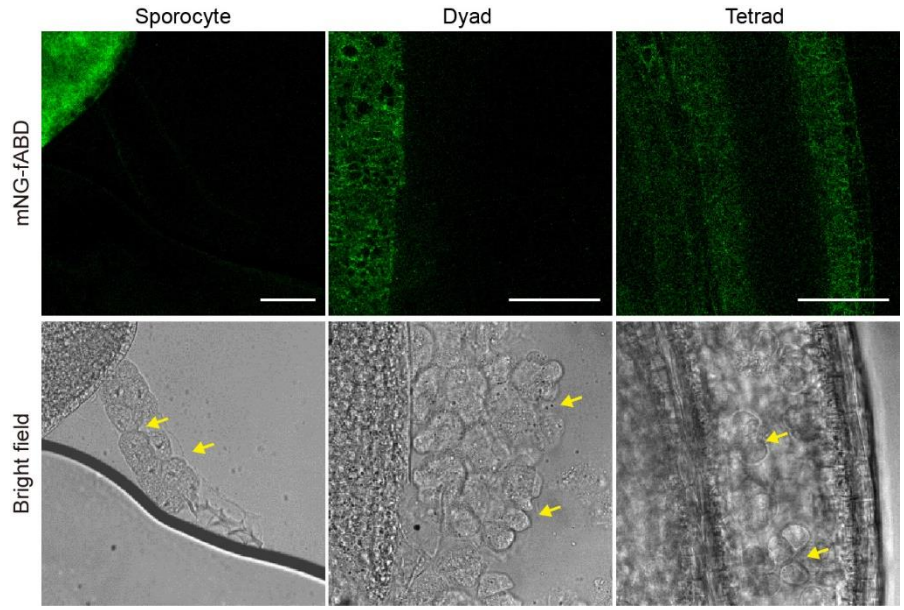

Fig. S2. RUBQ driven actin cytoskeleton signal is absent in pollen mother cells. Single images of young anthers from the mNG-fABD line. Arrows indicate the pollen mother cells where no clear green signals can be seen. Scale bars: 10 μm.

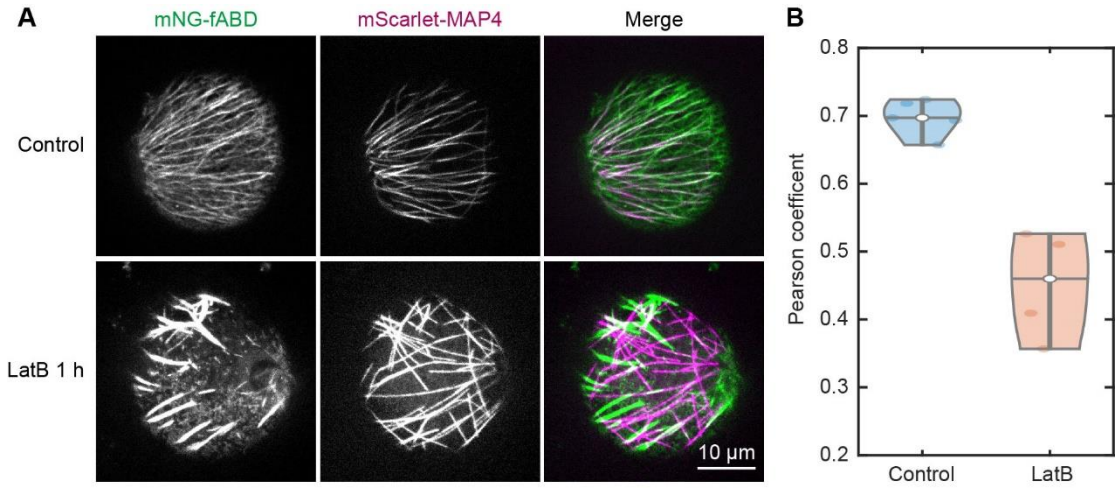

Fig. S3. Partial depolymerization of actin cytoskeleton decreased the interplay between actin and microtubule in rice pollen. (A) Maximum projected images of the cytoskeletons in pollen with/without LatB treatment. The pollen was treated with 1 μM actin inhibitor Latrunculin B for 1 h. Note the change of microtubules from radial alignment to more disordered alignment. (B) Pearson correlation coefficient between actin filaments and microtubules in the treatment in (A). 4 to 5 pollens were used for this analysis.

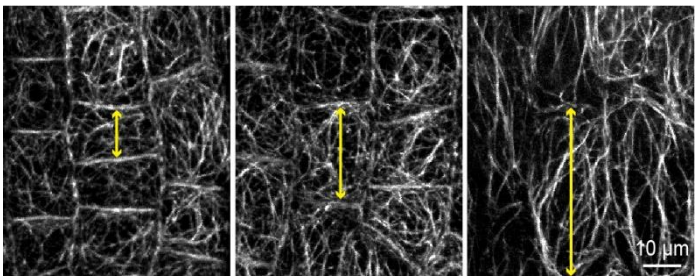

Fig. S4. Actin cytoskeleton reorientation in anther epidermis. Actin filaments in rice anther epidermis where the actin direction changes from disordered to longitudinal (from left to right) alignment. The increased cell length (indicating by yellow arrows) indicates the cell growth stage. The images are maximum projections.

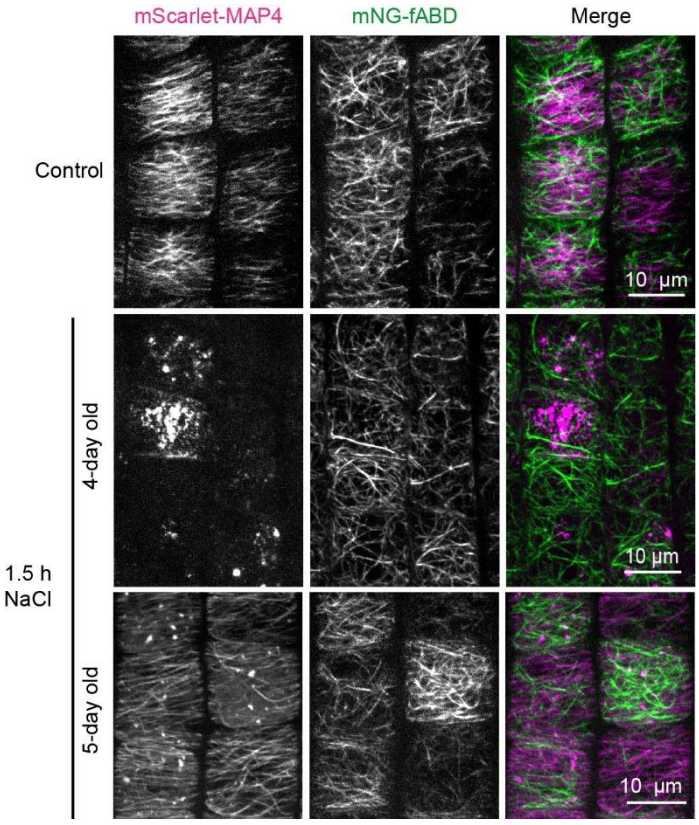

Fig. S5. Seedling age determines the sensitivity to salt treatment. Images of different age rice seedlings were treated with 250 mM NaCl. The images are maximum projections from root epidermis. Note that the difference of microtubule depolymerizing extent and microtubule-related foci number.

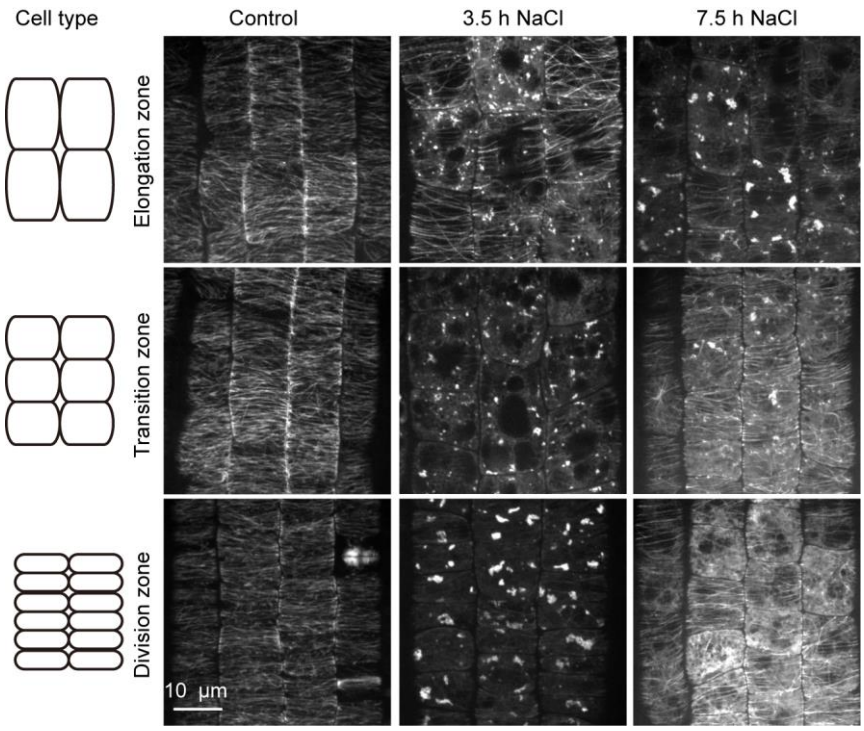

Fig. S6. The timing of microtubule response to salt differs in root cell types. Images of microtubule (mScarlet-MAP4) in different root epidermal cells. Schematic views of the cell shape at different zones are outlined in left panel. The root parts of five-day old seedlings were incubated with 250 mM NaCl for the indicated times. The images are maximum projections from z-stacks.

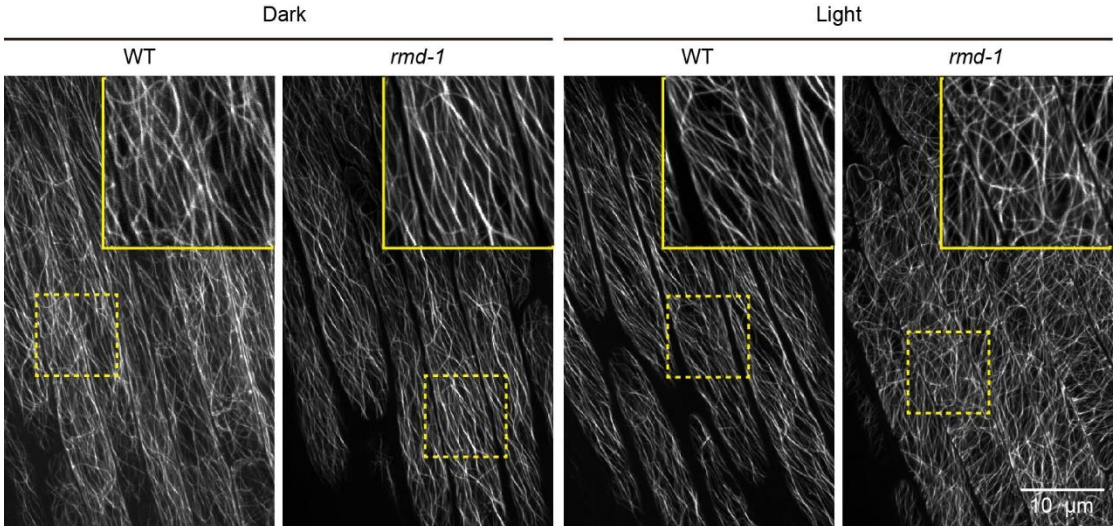

Fig. S7. The microtubule array in *rmd-1* coleoptile. The mNG-MAP4 seeds were germinated for 4 days under either dark or light condition. The images are maximum projections from epidermis. The enlargements' positons are indicated by the dashed rectangles in each large images.

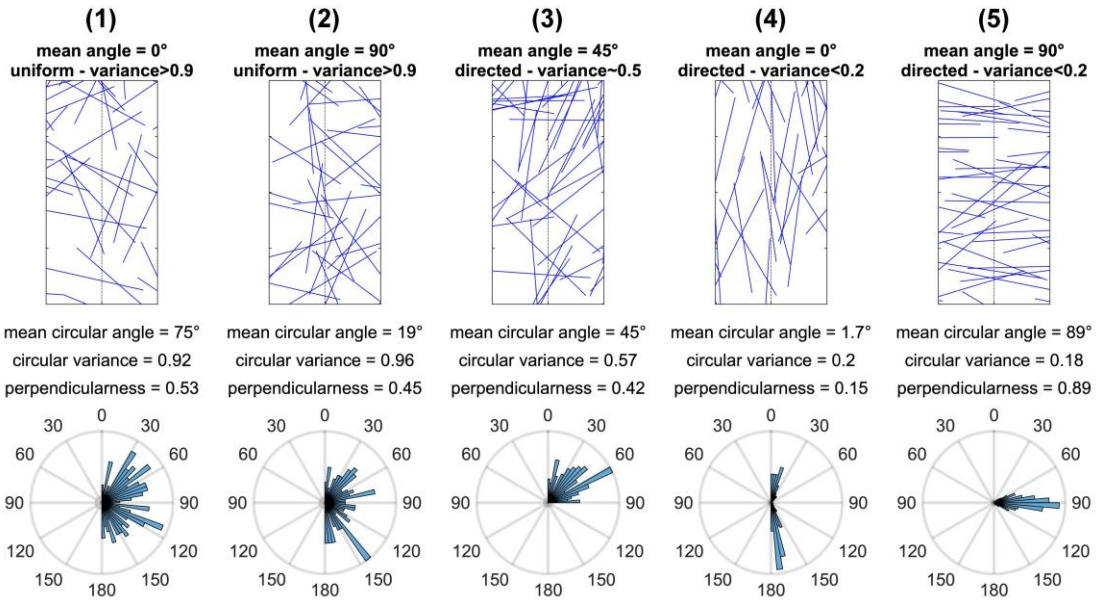

Fig. S8. Description of the circular statistics using simulated filament networks. Each column shows a simulated network (N=200; not all edges are shown) using random generated angles from a von-Mises distribution (the normal distribution in circular statistics; Berens, 2009; Fisher, 1993; Jammalamadaka and SenGupta, 2001). The values used in the simulations are: **(1)** μ=0°, κ=0; **(2)** μ=90°, κ=0; (**3)** μ=0°, κ=1; **(4)** μ=0°, κ=4; **(5)** μ=90°, κ=4. The dotted line indicates the major cell axis and all angles were restricted to 0°-180°in order to resemble edge angles that were extracted using Cytoseg2. More description is included in Materials and Methods section.

Table S1. The evaluation of rice cytoskeleton fluorescent marker constructs

Construct elements	Used elements	Evaluation
Promoter	35S	Gene silencing, usually high expression in stomata guard cells, no expression in reproductive tissues.
	ZmUbi1	Express in all tissues except pollen mother cell, no gene silencing observed.
	RUBQ2	Express in all tissues except pollen mother cell, no gene silencing observed. Expression level is higher than ZmUbi1.
Fluorescent protein	GFP	Good.
	mNeongreen	Best. Brighter than GFP.
	mScarlet	Bright but sensitive to photo-bleaching.
Actin binding protein	OsfABD	Not determined. (No signal was observed, not sure the reason)
	AtfABD	Label filamentous actin with quite dynamic.
Microtubule binding protein	OsTUA1	Weakly label microtubules in rice cells, mainly retained in cytosol, also cause plant distortion phenotype.
	MAP4	Microtubule labelling well. High expression sometimes caused plant dwarf phenotype. Normal plants can be obtained.

Table S2 The quantification of microtubule filaments in salt treated cell

Time point of salt treatment	Total filament counts	Number of analyzed cells	Mean filament per cell
1.5-2 h	1265	96	13.59
3.5-4 h	Not detectable	111	Not detectable
5.5-6 h	152	122	1.25
7.5-8 h	1903	138	13.79

Table S3. Statistical test of edge capacity using Mann–Whitney U test

Dataset	Wild type (dark)	*rmd-1* (dark)	Wild type (light)	*rmd-1* (light)
Wild type (dark)		p<0.001	p=0.005	p<0.001
rmd-1 (dark)	p<0.001		p<0.001	p<0.001
Wild type (light)	p=0.005	p<0.001		p<0.001
rmd-1 (light)	p<0.001	p<0.001	p<0.001	

* Green shading indicates significant difference with 95% confidence intervals (p<0.05)

Table S4. The used primers

Plasmid	Fragment	Primer sequence
RUBQ2/ ZmUbi::mNG-MAP4/ fABD	RUBQ2 promoter	FP ATGACCATGATTACGAATTCATTCGGGTCAAGGCGGAAGC RP GGTACCGAGCTCGAATTCCTGCAAGAAATAATCACCAA
	Zmubiquitin1 promoter	FP ATGACCATGATTACGCAGTGCAGCGTGACCCGGT RP TACCGAGCTCGAATTCGGATCCTCTAGAGTCGACCTGCAGA
	mNeongreen	FP ATTCGAGCTCGGTACCATGGTGAGCAAGGGCGA RP CGACTCTAGAGGATCCCTTGTACAGCTCGTC
	MAP4	FP GCTGTACAAGGATCCTCCCGGCAAGAAGAA RP ATTCGAGCTGGTCACCCTAGTCACCTCCTGA
	AtfABD	FP GCTGTACAAGGATCCTCTTGAAAGAGCTGAA RP ATTCGAGCTGGTCACCCTATTCGATGGATGC
RUBQ2:: mScarlet	mScarlet	FP TTCGAGCTCGGTACCATGGTGAGCAAGGGCGAGG MSCARLET-MAP4-RP TGCTTCTTCTTGCCGGGAGGATCCCTTGTACAGCTCGTC MSCARLET-FABD-RP ATTCAGCTCTTTCAAGAGGATCCCCTTGTACAGCTCGTC
ZmUbi::GFP-OsTUA1/ OsfABD	GFP	FP ATTCGAGCTCGGTACCATGGTGAGCAAGGGCGAGGA RP CTAGAGGATCCCCGGGTACCCTTGTACAGCTCGTCCATGCC
	OsTUA1	FP GCAGGCATGCAAGCTTATGAGGGAGTGCATCTCGAT RP TCACCTGTAATTCACACGTGCTAGTACTCGTCACCATCATCGC
	OsfABD	FP GCAGGCATGCAAGCTTTTCCTCAAGTCCAGTACCA RP TCACCTGTAATTCACACCTAAAGAATTAAATGAGGCCTT
35S::GFP-AtfABD/MAP4	GFP	FP CGGGGGACTCTTGACCATGGTGAGCAAGGGCGAGGA RP CCTCAGATCTACCATGCTTGTACAGCTCGTCCATGC
	AtfABD	FP AAGCATGGTAGATCTCTTGAAAGAGCTGAA RP ATTCGAGCTGGTCACCCTATTCGATGGATGCTTCCTCTGAG
	MAP4	FP AAGCATGGTAGATCTTCCCGGCAAGAAGAA RP ATTCGAGCTGGTCACCCTAGTCACCTCCTGA

Note: The homogenous sequence for infusion is underlined.

Movie 1. The time-lapse movie of mNG-MAP4 in rice coleoptile, related to Fig. 2C.

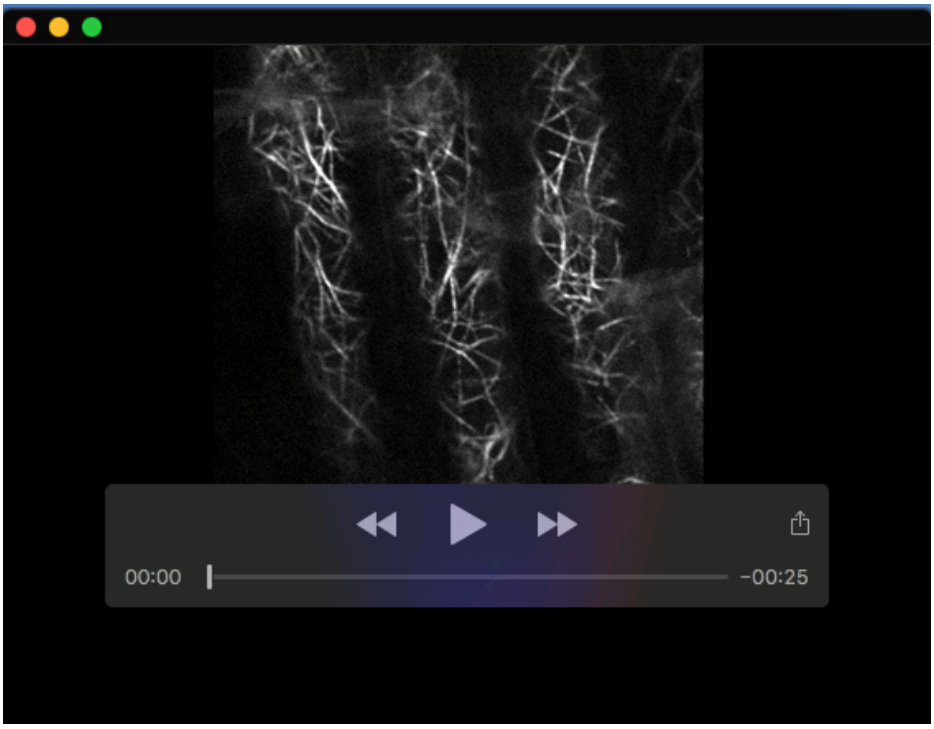

Movie 2. The time-lapse movie of mNG-fABD in rice coleoptile, related to Fig. 2E.

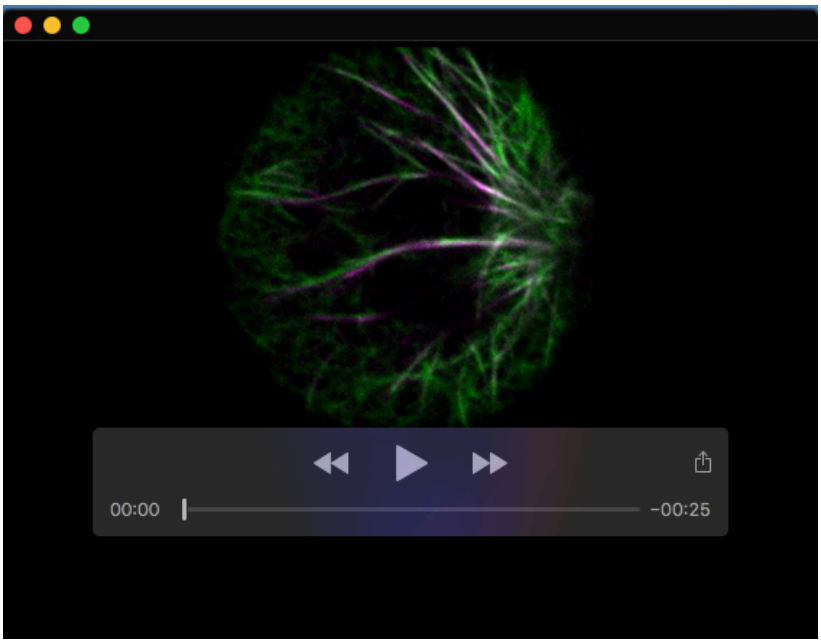

Movie 3. The time-lapse movie of mNG-fABD mScarlet-MAP4 in rice pollen, related to Fig. 4D. Please note the co-migration between two signals. mNG-fABD is in green and mScarlet-MAP4 is in magenta.

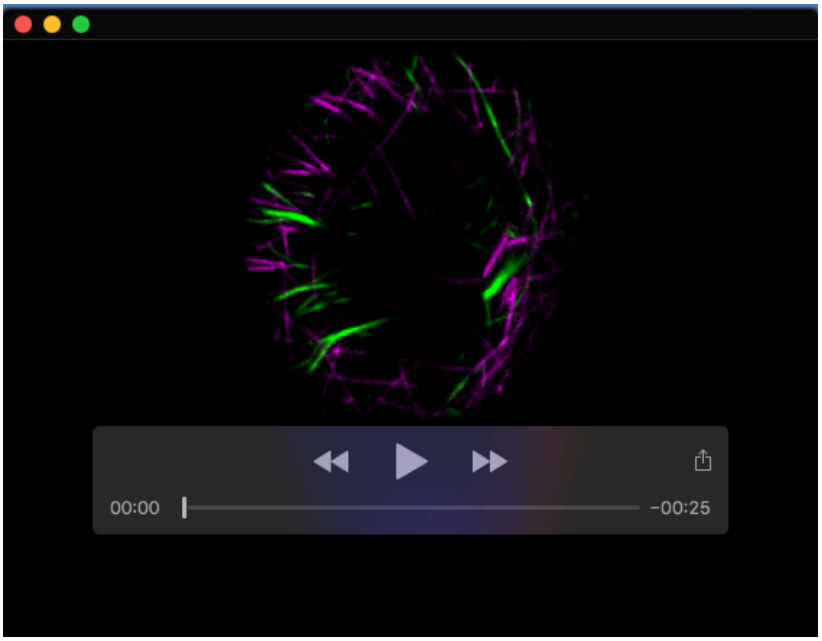

Movie 4. The time-lapse movie of mNG-fABD mScarlet-MAP4 in rice pollen treated with Latrunculin B, related to Fig. 4G. Please note the signal changes along the time.

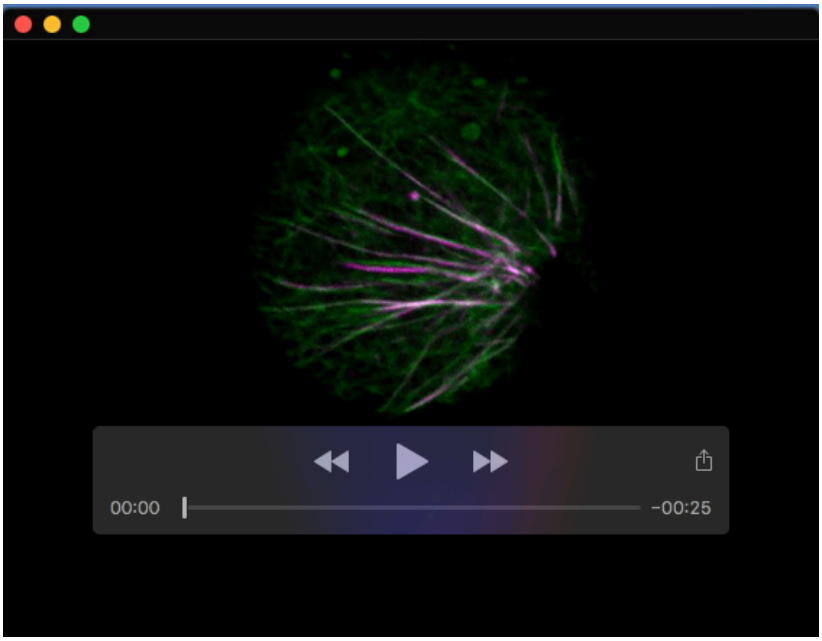

Movie 5. The time-lapse movie of mNG-fABD mScarlet-MAP4 in rice pollen treated with oryzalin, related to Fig. 4H. Please note the signal changes along the time.

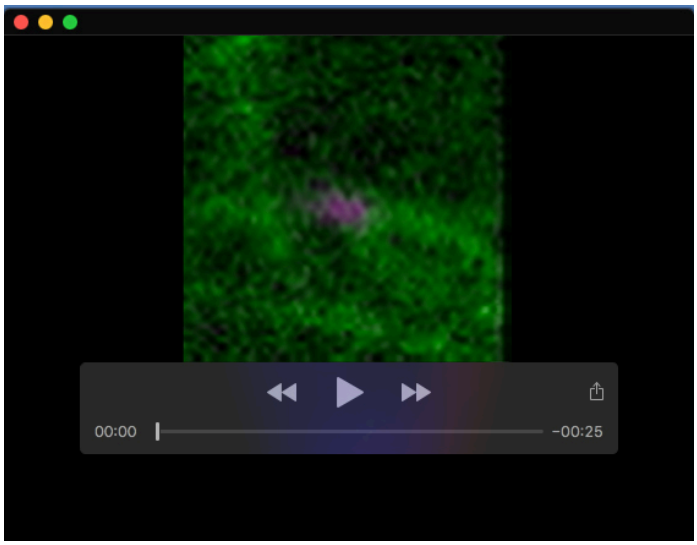

Movie 6. The time-lapse movie of mNG-fABD mScarlet-MAP4 in rice root treated with 250 mM NaCl for 1.5 h, related to Fig. 7B. Time interval is 10 sec.

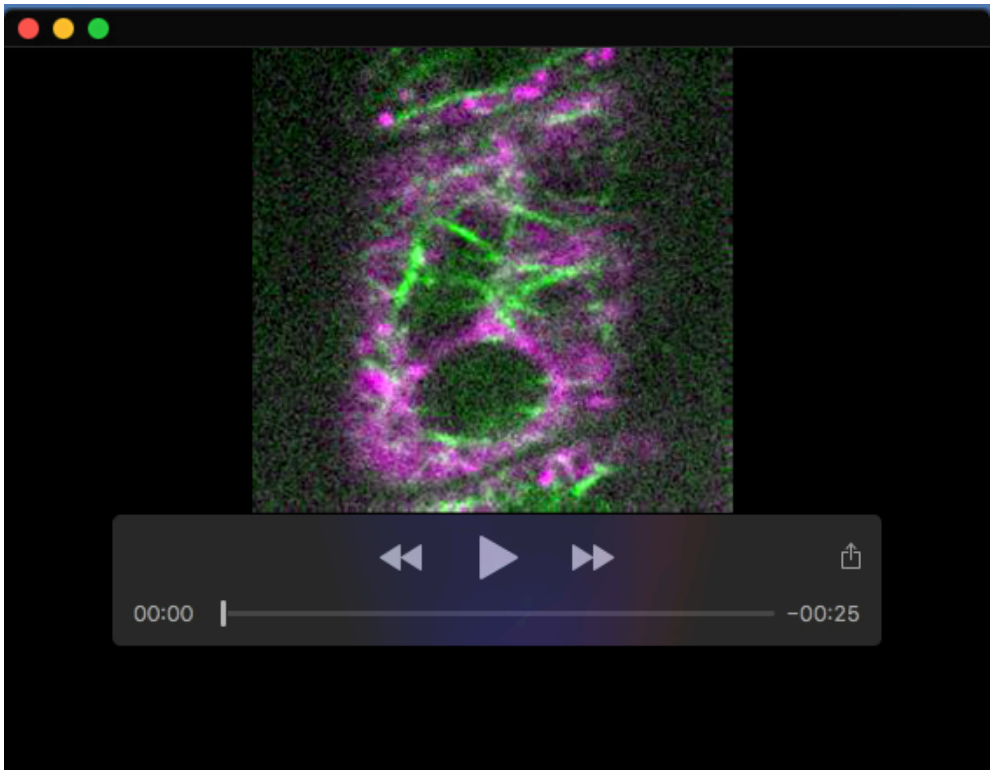

Movie 7. The time-lapse movie of mNG-fABD mScarlet-MAP4 in rice root treated with 250 mM NaCl for 5 h, related to Fig. 7D. Time interval is 10 sec.